pH-Responsive Non-ionic Diblock Copolymers: Protonation of a Morpholine End-group Induces an Order-Order transition

N. J. W. Penfold[a], J. R. Lovett[a], N. J. Warren[a], P. Verstraete[b], J. Smets[b] and S. P. Armes[a]

[a]Department of Chemistry, University of Sheffield, Brook Hill, Sheffield, South Yorkshire, S3 7HF
[b]Procter & Gamble, Temselaan 100, 1853 Strombeek Bever, Belgium

Abstract

A new morpholine-functionalised, trithiocarbonate-based RAFT agent, MPETTC, was synthesised with an overall yield of 80% and used to prepare a poly(glycerol monomethacrlyate) (PGMA) chain transfer agent. Subsequent chain extension with 2-hydroxypropyl methacrylate (HPMA) using a RAFT aqueous dispersion polymerisation formulation at pH 7.0 – 7.5 resulted in the formation of morpholine-functionalised PGMA-PHPMA diblock copolymer worms via polymerisation-induced self-assembly (PISA). These worms form soft, free-standing aqueous hydrogels at 15% w/w solids. Acidification causes protonation of the morpholine end-groups at pH 3, which increases the hydrophilic character of the PGMA stabiliser block. This causes a subtle change in the copolymer packing parameter which induces a *worm-to-sphere* morphological transition and hence leads to *in situ* degelation. This order-order transition was characterised by dynamic light scattering (DLS), transmission electron microscopy (TEM) and gel rheology studies. On returning to pH 7, regelation is observed at 15% w/w solids, indicating the reversible nature of the transition. However, such diblock copolymer worm gels remain intact when acidified in the presence of electrolyte, since the cationic surface charge arising from the protonated morpholine end-groups is screened under these conditions. Moreover, *regelation* is also observed in relatively acidic solution (pH < 2), because the excess acid acts as a salt under these conditions and so induces a *sphere-to-worm* transition.

Introduction

Block copolymer self-assembly has become one of the most important fields in polymer chemistry over the last few decades.[1-20] The synthesis of functional block copolymers is not trivial by classical living ionic polymerisation techniques, since many groups (-OH, -COOH, -NH_2 etc.) lead to premature termination via proton abstraction. However, the development of pseudo-living radical polymerisation techniques, such as atom transfer radical polymerisation (ATRP)[21, 22] and reversible addition-fragmentation chain transfer polymerisation (RAFT)[23] revolutionised the design and synthesis of functional block copolymers over the past two decades.[24, 25] In particular, the development of robust RAFT-mediated polymerisation-induced self-assembly (PISA) formulations offers a highly convenient route for the preparation of a wide range of well-defined amphiphilic diblock copolymer nano-objects directly in aqueous media.[26] Initially, a macromolecular chain transfer agent (macro-CTA) is synthesised and then this soluble precursor is chain-extended via aqueous dispersion (or aqueous emulsion) polymerisation.[27-30] Self-assembly occurs *in situ* as the growing second block becomes insoluble.[31] Depending on the precise

reaction conditions, this enables the reproducible formation of spheres, worms or vesicles at relatively high solids (25-50 % w/w).[27, 32]

In the case of RAFT aqueous emulsion polymerisation, kinetically-trapped spheres[27, 33, 34] are often obtained when the targeted diblock copolymer composition might be expected to favour worms or vesicles.[35-37]

In contrast, RAFT aqueous dispersion polymerisation usually provides access to all three copolymer morphologies, provided that the stabiliser macro-CTA is not so long as to impede sphere-sphere fusion.[38] Moreover, phase diagrams can be constructed for any given macro-CTA that enable pure copolymer phases to be consistently targeted for these latter formulations.[32, 39] The versatility of PISA has been exploited to synthesise non-ionic, cationic, anionic and zwitterionic diblock copolymer nano-objects directly in water.[39-46] A recent review by Warren and Armes summarises recent PISA syntheses via RAFT aqueous dispersion polymerisation.[38] The final block copolymer morphology is determined by the dimensionless packing parameter, *P*, which describes the relative volume fractions of the solvophilic stabiliser and solvophobic core-forming blocks.[31] When $P \leq {}^{1}/_{3}$, a spherical micelle morphology is favoured. If *P* lies in the range between ${}^{1}/_{3} \leq P \leq {}^{1}/_{2}$ then worms (a.k.a. cylinders) are produced, and vesicles are obtained when ${}^{1}/_{2} \leq P \leq 1$. The diblock copolymer worms are of particular interest, because they typically form soft, free-standing aqueous hydrogels, presumably as a result of multiple inter-worm contacts.[47] Moreover, some examples of worms exhibit stimulus-responsive behaviour. For example, Blanazs and co-workers reported that poly(glycerol monomethacrylate)-poly(2-hydroxypropyl methacrylate) (PGMA-PHPMA) diblock copolymer worms form thermo-responsive gels.[47, 48] Variable temperature rheology and ^{1}H NMR experiments confirmed that degelation occurred on cooling from 25 °C to 4-5 °C as a result of surface plasticisation (hydration) of the PHPMA cores, which induces a worm-to-sphere transition, as confirmed by transmission electron microscopy (TEM) and small-angle X-ray scattering (SAXS) studies. Heating the free-flowing dispersion of PGMA-PHPMA spheres from 4-5 °C up to 25 °C induces a sphere-to-worm transition, resulting in formation of a new worm gel with a modulus comparable to that of the original worm gel. These PGMA-PHPMA block copolymer worms are both biocompatible and readily sterilisable,[48] and are now being evaluated for potential use as a 3D medium for the long-term storage of human stem cells.[48] In this context, cell recovery from the gels is aided by their thermo-responsive (de)gelation behaviour.

Block copolymer nano-objects comprising of either weak polyacids or weak polybases have been utilised as pH-responsive vehicles for encapsulation anti-cancer drugs.[49-51] Such polyelectrolytic chains also enable the design of 'schizophrenic' spherical micelles and vesicles, which are capable of forming two (or even three) self-assembled nano-structures in aqueous solution as a function of pH.[52-56]

The effects of polymer end-groups have been studied by the examination of temperature and pH as external triggers. For example, the aqueous solution behaviour of both a poly(2-hydroxyethyl methacrylate) homopolymer prepared with a *N*-morpholine ATRP initiator[57] and a series of carboxylic acid terminated poly(*N*-isopropylacrylamide) (PNIPAM) oligomers[58] were each shown to depend on solution pH. In addition, Stöver et al. have shown that the lower critical solution temperature (LCST) of PNIPAM can be tuned by varying the nature of its end-groups.[59] Moreover, PNIPAM-stabilised block copolymer spheres prepared with a quaternary amine-based CTA undergo a sphere-to-worm transition when heated above the LCST of PNIPAM.[60] Here the permanently cationic end-group confers colloidal stability and so prevents macroscopic precipitation at higher temperatures.

Very recently, Lovett and co-workers utilised a carboxylic acid-based RAFT agent to prepare $PGMA_{56}$-$PHPMA_{155}$ diblock copolymer worms. On switching the solution pH from 3.5 to 7.0, these ostensibly *non-ionic* diblock copolymer worms

undergo a reversible worm-to-sphere transition, with concomitant degelation.[61] Dynamic light scattering (DLS), TEM and rheological studies confirm that ionisation of a *single* carboxylic acid group located at the end of each PGMA stabiliser chain is responsible for this unexpected pH-responsive behaviour. The packing parameter, *P*, is reduced as the carboxylic acid end-group becomes ionised, thus inducing a worm-to-sphere transition that results in complete degelation. More specifically, the gel storage modulus (*G'*) is dramatically reduced from ≈ 10^2 Pa at pH 3.7 to ≈ 0.02 Pa at pH 6.9. Returning to pH 3.7 leads to reprotonation of the anionic carboxylate end-groups; this induces a sphere-to-worm transition that results in regelation, with the reconstituted worm gel possessing a comparable modulus to that of the original worm gel.

In the present work, we describe the synthesis of a new morpholine-functional trithiocarbonate-based RAFT chain transfer agent (MPETTC, see Scheme 1). This CTA is used to prepare tertiary amine-functionalised PGMA-PHPMA diblock copolymer worms that are expected to exhibit *complementary* pH-responsive behaviour to that reported by Lovett et al.[61] (Scheme 2). This hypothesis is examined using TEM, DLS, aqueous electrophoresis and rheology.

Experimental

Materials

Glycerol monomethacrylate (GMA; 99.8%; < 0.06 mol % dimethacrylate impurity) was kindly donated by GEO Specialty Chemicals (Hythe, UK) and used without further purification. 2-Hydroxypropyl methacrylate (HPMA; 97%), 2,2'-azobis(2-methylpropionamidine) dihydrochloride (AIBA; 99%), *N*-hydroxyl succinimide (98%), *N,N'*-dicyclohexylcarbodiimide (99%) and 4-(dimethylamino)pyridine (99%) were purchased from Sigma Aldrich and were used as received. 4-(2-Aminoethyl)morpholine (99%) was purchased from Sigma Aldrich (UK) and distilled under vacuum before use. All other chemicals and solvents were purchased from either VWR Chemicals or Sigma Aldrich and were used as received, unless otherwise stated. Anhydrous dichloromethane and chloroform were obtained from an in-house Grubbs purification system.

^{1}H NMR spectroscopy

NMR spectra were recorded at ambient temperature using a 400 MHz Bruker AV3-HD spectrometer in CD_3OD (for calculation of monomer conversions and mean degrees of polymerisation, DPs) and CD_2Cl_2 or $CDCl_3$ (for RAFT agent synthesis). All chemical shifts are reported in ppm (δ).

Dynamic light scattering (DLS)

DLS and aqueous electrophoresis measurements were conducted at 20 °C using a Malvern Instruments Zetasizer Nano series instrument equipped with a 4 mW He−Ne laser (λ = 633 nm) and an avalanche photodiode detector. Scattered light was detected at 173°. Copolymer dispersions were diluted using an aqueous solution of 1 mM KCl to a final concentration of 0.1% w/w solids and the pH was adjusted using HCl or KOH, as required. Intensity-average hydrodynamic diameters were calculated via the Stokes-Einstein equation. Zeta potentials were calculated from the Henry equation using the Smoluchowski approximation.

Gel permeation chromatography (GPC)

0.50% w/w copolymer solutions were prepared in DMF containing DMSO (10 µL mL^{-1}) as a flow rate marker. GPC measurements were conducted using HPLC-grade DMF eluent containing 10 mM LiBr at 60 °C at a flow rate of 1.0 mL min^{-1}. A Varian 290-LC pump injection module was connected to two Polymer Laboratories PL gel 5 µm Mixed-C columns connected in series and a Varian 390-LC multi-detector suite (refractive index detector). Sixteen near-monodisperse poly(methyl methacrylate) standards ranging from M_p = 645 g mol^{-1} to 2,480,000 g mol^{-1} were used for calibration.

Transmission electron microscopy (TEM)

Copper/palladium grids were surface-coated in-house to produce a thin film of amorphous carbon and then plasma glow-discharged for 20 seconds to produce a hydrophilic surface. Droplets (10 µL) of freshly-prepared 0.1% w/v aqueous copolymer dispersions of the desired solution pH were placed on the hydrophilic grid for 30 seconds, blotted to remove excess solution and then negatively stained with uranyl formate solution (0.75% w/v) for a further 30 seconds. Excess stain was removed by blotting and each grid was carefully dried with a vacuum hose. TEM grids were imaged using a FEI Tecnai Spirit microscope fitted with a Gatan 1kMS600CW CCD camera operating at 80 kV.

Rheology measurements

An AR-G2 rheometer equipped with a variable temperature Peltier plate and a 40 mm 2° aluminium cone was used for all rheological experiments. Percentage strain and angular frequency sweeps were conducted at pH 7 and 20 °C. The storage modulus (*G*') and loss modulus (*G*'') were determined at 15% w/w, 20 °C as a function of dispersion pH at an applied strain of 1.0 % and a frequency of 1.0 rad s^{-1}.

Synthesis of SPETTC

4-cyano-4-(2-phenylethanesulfanyl-thiocarbonyl)sulfanyl-pentanoic acid (PETTC) was synthesised in-house according to previous protocols.62 All glassware was dried in a 150 °C oven overnight, then flame-dried under vacuum before use to remove trace water. A 50 mL, one-neck round-bottom flask was charged with PETTC (1.60 g, 4.71 mmol) and N-hydroxyl succinimide (0.54 g, 4.71 mmol) which were then dissolved in anhydrous dichloromethane (20.0 g, 15.0 mL). N,N'-dicyclohexylcarbodiimide (0.97 g, 4.71 mmol) was added and then stirred in the dark for 16 h. The insoluble N,N'-dicyclohexylurea was removed by filtration. The organic solution was washed with water (4 x 10 ml), dried with MgSO4, concentrated under vacuum and purified by recrystallisation from a 4:1 (v/v) ethyl acetate/hexane mixture to yield 4-cyano-4-(2-phenylethanesulfanylthiocarbonyl)sulfanyl pentanoic succinimide ester (SPETTC, 1.90 g, 92% yield) 1H NMR (400 MHz, CD2Cl2, 25 °C): δ 1.89 (s, 3H, -(CN)CH3), 2.51 – 2.68 (m, 2H, -(CH3)(CN)CH2CH2C(=O)O), 2.81 (s, 4H, -(C=O)(CH2)2(C=O), 2.90 – 2.96 (t, 2H, -(CH3)(CN)CH2CH2C(=O)), 2.97 – 3.03 (t, 2H, -PhCH2CH2S(C=S)S), 3.56 – 3.64 (t, 2H, PhCH2CH2S(C=S)S), 7.20 -

7.36 (m, 5H, -PhCH2CH2S(C=S)S). 13C NMR (400 MHz, CDCl3, 25 °C): δ 24.8 (CH3), 25.7 (C(=O)(CH2)2C(=O)), 26.9 (CH2CH2C(=O)ON),, 33.2 (Ph*C*$H_2$$CH_2$S), 34.1 (*C*$H_2$$CH_2$C(=O)O), 38.1 (PhCH$_2$*C*$H_2$S), 46.2 (S*C*($CH_3$)(CN)$CH_2$), 118.7 SC($CH_3$)(*C*N)$CH_2$), 126.9, 128.6, 128.8, 139.2 (*Ph*CH_2), 167.2 (*C*=O), 168.9 (*C*(=O)$(CH_2)_2$*C*(=O)), 216.4 (*C*=S). HRMS (ES^+) *m/z* calcd: 437.0658 Found: 437.0658 Anal. Calcd for $C_{19}H_{20}N_2O_4S_3$: C, 52.27; H, 4.62; N, 6.42; S, 22.03 Found: C, 52.65; H, 4.72; N, 6.39; S, 21.93.

Synthesis of MPETTC

All glassware was dried in a 150 °C oven overnight, then flame-dried under vacuum before use to remove traces of water. A 500 ml one-neck round-bottom flask containing a magnetic stirrer bar was charged with SPETTC (5.35 g, 12.3 mmol), which was dissolved in anhydrous chloroform (250 mL). In a separate 50 ml one-neck round-bottom flask, freshly distilled 4-(2-aminoethyl)morpholine (1.52 g, 1.53 mL, 11.7 mmol) was dissolved in anhydrous chloroform (25 mL), then added in one portion to the solution of SPETTC. The yellow reaction mixture was heated at 30 °C for 90 min, filtered and washed with saturated $NaHCO_3$ solution (3 x 400 mL) to remove residual *N*-hydroxysuccinimide, before being dried with $MgSO_4$. After solvent removal, the yellow oil was purified to remove any residual SPETTC via column chromatography using silica gel 60 (Merck) as the stationary phase and a 95:5: v/v dichloromethane/methanol mixed eluent, followed by drying in a vacuum oven overnight to isolate a viscous yellow oil (MPETTC, 4.75 g, 86%). ^{1}H NMR (400 MHz, CD_2Cl_2, 25 °C): δ 1.89 (s, 3H, -(CN)C***H$_3$***), 2.31 – 2.56 (m, 10H, see Figure. 1 for assignment), 2.96 – 3.03 (t, 2H, -PhC***H$_2$***CH_2S(C=S)S), 3.27 – 3.34 (q, 2H, C(=O)NHC***H$_2$***CH_2), 3.56 – 3.62 (t, 2H, PhCH$_2$C***H$_2$***S(C=S)S), 3.64 – 3.71 (t, 4H, -CH_2NCH$_2$C***H$_2$***O) 5.98 – 6.13 (s, 1H, CON***H***), 7.20 - 7.36 (m, 5H, -***Ph***$CH_2$$CH_2$S(C=S)S). ^{13}C NMR (400 MHz, $CDCl_3$, 25 °C): δ 25.1 (***CH$_3$***), 31.8 (CH_2***CH$_2$***CONH), 34.6 (Ph***CH$_2$***CH_2S), 34.5 (***CH$_2$***CH_2CONH) , 35.7 (CONH***CH$_2$***CH_2N), 37.9 (PhCH$_2$***CH$_2$***S), 46.8 (S***C***(CH_3)(CN)CH_2), 53.3 (-N***CH$_2$***CH_2O), 56.9 (CONHCH$_2$***CH$_2$***N), 66.9 (-NCH$_2$***CH$_2$***O), 119.2 (SC(CH_3)(***CN***)CH_2), 126.8, 128.5, 128.7, 139.1 (***Ph***CH_2), 170.1 (***C=O***), 216.8 (***C=S***). HRMS (ES^+) *m/z* calcd: 452.1495 Found: 452.1495. Anal. Calcd for $C_{21}H_{29}N_3O_2S_3$: C, 55.85; H, 6.47; N, 9.30; S, 21.29. Found: C, 55.47; H, 6.48; N, 9.08; S, 21.09.

Synthesis of MPETTC-poly(glycerol monomethacrylate) macro-CTA by RAFT solution polymerisation in ethanol

A 100 ml round-bottom flask was charged with a magnetic stirrer bar, glycerol monomethacrylate (GMA, 18.9 g, 118 mmol), MPETTC RAFT agent (0.76 g, 1.70 mmol; target DP = 70), AIBA (92.0 mg, 0.34 mmol; [MPETTC]/[AIBA] molar ratio = 5.0) and ethanol (24.2 g, 30.6 mL) to afford a 45% w/w orange solution. The flask was sealed, placed in an ice bath and degassed under N_2 for 30 min at 0 °C, before being placed in a preheated oil bath set at 56 ^{o}C for 2 h. The GMA polymerisation was quenched by exposure to air while cooling to 20 °C. ^{1}H NMR indicated 61% monomer conversion by comparison of the integrated methacrylic backbone signals at 3.70 – 4.30 ppm to that of the GMA vinyl signals at 6.14 – 6.20 ppm. Purification was achieved by precipitation into a twenty-fold excess of dichloromethane to remove unreacted GMA monomer, followed by filtration. The crude PGMA was redissolved in the minimum amount of methanol and precipitated a second time using a ten-fold excess dichloromethane, with isolation via filtration. Purified PGMA macro-CTA was dissolved in water, placed on a

rotary evaporator to remove residual dichloromethane, and then freeze-dried for 48 h to afford a yellow powder. ^{1}H NMR studies indicated no residual GMA monomer and a mean degree of polymerisation of 50 was determined via end-group analysis, with a RAFT agent efficiency of 85%. DMF GPC studies indicated an M_n of 12,800 g mol^{-1} and an M_w/M_n of 1.20 against near-monodisperse poly(methyl methacrylate) standards.

Synthesis of MPETTC-PGMA$_{50}$-PHPMA$_{140}$ diblock copolymer worms by RAFT Aqueous Dispersion Polymerisation

A typical protocol for the synthesis of PGMA50-PHPMA140 diblock copolymers by RAFT aqueous dispersion polymerisation was conducted as follows. PGMA50 macro-CTA (0.80 g, 94.7 µmol), HPMA monomer (1.90 g, 13.2 mmol; target DP = 140), AIBA (5.10 mg, 18.8 µmol; PGMA50 macro-CTA/AIBA molar ratio = 5.0) and H2O (15.3 mL) were added to a 50 mL round-bottomed flask to afford a 15% w/w solution. The solution pH was adjusted from pH 6.5 to pH 7.0-7.5 using 0.1 M KOH. The sealed reaction flask was placed in an ice bath and degassed under N2 for 30 min at 0 °C, then placed in a preheated oil bath set at 56 °C for 3 h. The HPMA polymerisation was quenched by exposure to air while cooling to 20 °C. The resulting diblock copolymer worm gel was characterised by 1H NMR, DLS, TEM and gel rheology experiments.

Synthesis of MePETTC

MePETTC was synthesised according to a previous protocol.[61] A 25 mL round-bottomed flask was flame-dried under vacuum and cooled to 20 °C, then charged with a magnetic stirrer bar, PETTC RAFT agent (0.56 g, 1.65 mmol) and anhydrous dichloromethane (5.60 g, 4.20 mL). The flask was immersed in an ice bath to 0 °C for 5 min. DMAP (45.0 mg, 0.37 mmol) and excess methanol (0.28 g, 8.74 mmol) were added and then *N,N'*-dicyclohexylcarbodiimide (0.36 g, 1.73 mmol) was gradually added over 5 min. The reaction was stirred overnight at 20 °C. *N,N'*-Dicyclohexylurea was isolated via filtration and the crude product was purified by column chromatography (silica gel 60, using dichloromethane eluent) and dried in a vacuum oven overnight to isolate a viscous yellow oil (MePETTC, 4.75 g, 89%) ^{1}H NMR (400 MHz, CD_2Cl_2, 25 °C) δ 1.86 (s, 3H, -(CN)C***H*****$_3$**), 2.32–2.61 (m, 2H, -(CH_3)(CN)C***H*****$_2$**CH_2COOMe), 2.64–2.74 (t, 2H, -(CH_3)(CN)CH_2C***H*****$_2$**COOMe), 2.96–3.05 (t, 2H, -PhC***H*****$_2$**CH_2S(C=S)S)**,** 3.56 – 3.63 (t, 2H, PhCH_2C***H*****$_2$**S(C=S)S), 3.68 (s, 3H, -COOC***H*****$_3$**), 7.20 – 7.36 (m, 5H, -***Ph***CH_2CH_2S(C=S)S). ^{13}C NMR (400 MHz, $CDCl_3$, 25 °C): . HRMS (ES^+) *m/z* calcd: 354.0651 Found: 354.0651. Anal. Calcd for $C_{16}H_{19}NO_2S_3$: C, 54.36; H, 5.42; N, 3.96; S, 27.21. Found: C, 53.92; H, 5.21; N, 3.34; S, 27.40

Synthesis of MePETTC-PGMA$_{58}$ macro-CTA by RAFT Solution Polymerisation

A 25 mL round-bottomed flask was charged with GMA (4.65 g, 29.0 mmol), MePETTC (0.146 g, 0.416 mmol), AIBA (22.3 mg, 82.4 µmol) and ethanol (5.90 g, 7.47 mL) to afford a 45% wt. orange solution (target DP = 70, [MePETTC]/[AIBA] molar ratio = 5.0). The flask was sealed, placed in an ice bath and degassed under N_2 for 30 min at 0 °C. The flask was placed in a preheated oil bath set at 56 °C for 2 h. The GMA polymerisation was quenched by exposure to air and cooling to 20 °C. ^{1}H NMR indicated 58% monomer conversion by comparison of the integrated methacrylic backbone signals at 3.70 – 4.30 ppm to that of the GMA vinyl signals at 6.14 – 6.20 ppm. Purification was achieved by precipitation into a twenty-fold excess of

dichloromethane to remove unreacted GMA monomer, followed by filtration. The isolated crude PGMA was redissolved in the minimum amount of methanol, precipitated using a ten-fold excess of dichloromethane and again isolated via filtration. The purified macro-CTA was dissolved in water, residual dichloromethane was removed under reduced pressure using a rotary evaporator and then freeze-drying was conducted for 48 h to afford a yellow powder. ^{1}H NMR studies indicated no residual GMA monomer and end-group analysis indicated a mean degree of polymerisation of 58, with a RAFT agent efficiency of 70%. DMF GPC studies indicated an M_n of 14,600 g mol^{-1} and an M_w/M_n of 1.23 against a series of ten near-monodisperse poly(methyl methacrylate) calibration standards.

Synthesis of MePETTC-PGMA$_{58}$-PHPMA$_{160}$ diblock copolymer worms by RAFT Aqueous Dispersion Polymerisation

A typical protocol for the synthesis of a PGMA$_{58}$-PHPMA$_{160}$ diblock copolymer by RAFT aqueous dispersion polymerisation was conducted as follows. PGMA$_{58}$ macro-CTA (0.10 g, 10.4 µmol), HPMA monomer (0.24 g, 1.66 mmol; target DP = 160), AIBA (0.56 mg, 2.07 µmol; PGMA$_{58}$ macro-CTA/AIBA molar ratio = 5.0) and H_2O (1.95 mL) were added to a 10 mL round-bottom flask to afford a 15% w/w solution. The solution pH was adjusted from pH 6.5 to pH 7.0-7.5 with 0.1 M KOH and stirred for 5 minutes. The sealed reaction flask was placed in an ice bath and degassed under N_2 for 20 minutes at 0 °C, then placed in a preheated oil bath set at 56 °C for 3 h. Polymerisation was quenched by cooling to room temperature while exposing to air. Diblock copolymer worm gels were characterised by ^{1}H NMR, DLS, TEM and rheological experiments.

Results and Discussion

Bathfield and co-workers reported the modification of a carboxylic acid functionalised RAFT agent with 4-(2-aminoethyl)morpholine as a model compound to assess the feasibility of attaching amino derivatives of carbohydrates and biotin to RAFT agents.[63] Amines react preferentially with succinimidyl esters compared to RAFT dithioester or trithiocarbonate groups. Nevertheless, the amine/succinimidyl ester molar ratio was maintained below unity in the present study in order to maximise RAFT agent fidelity.[63, 64] The derivatisation of PETTC was monitored by ^{1}H NMR spectroscopy in CD_2Cl_2. PETTC has four distinct proton environments for its eight methylene protons between 2 and 4 ppm (Figure 1, black trace). The succinimidyl ester intermediate, SPETTC, was prepared in 86% yield (Scheme 1a).

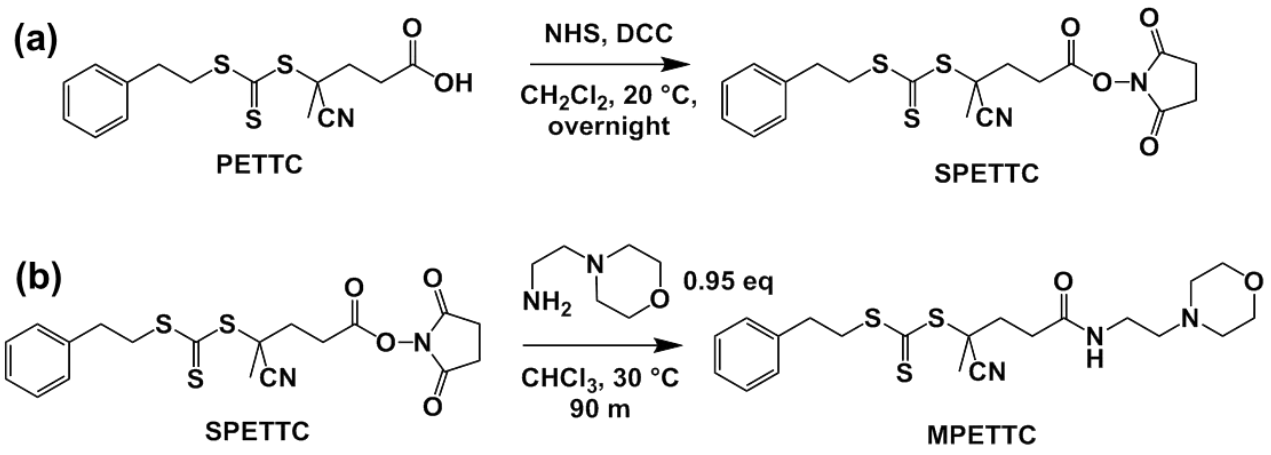

Scheme 1 Two-step synthesis of the MPETTC RAFT agent: (a) PETTC is converted into the corresponding succinimide ester, SPETTC; (b) this intermediate is then reacted with 4-(2-aminoethyl)morpholine to produce the desired MPETTC. Other reagents: NHS = *N*-hydroxylsuccinimide, DCC = *N, N'*-dicyclohexylcarbodiimide.

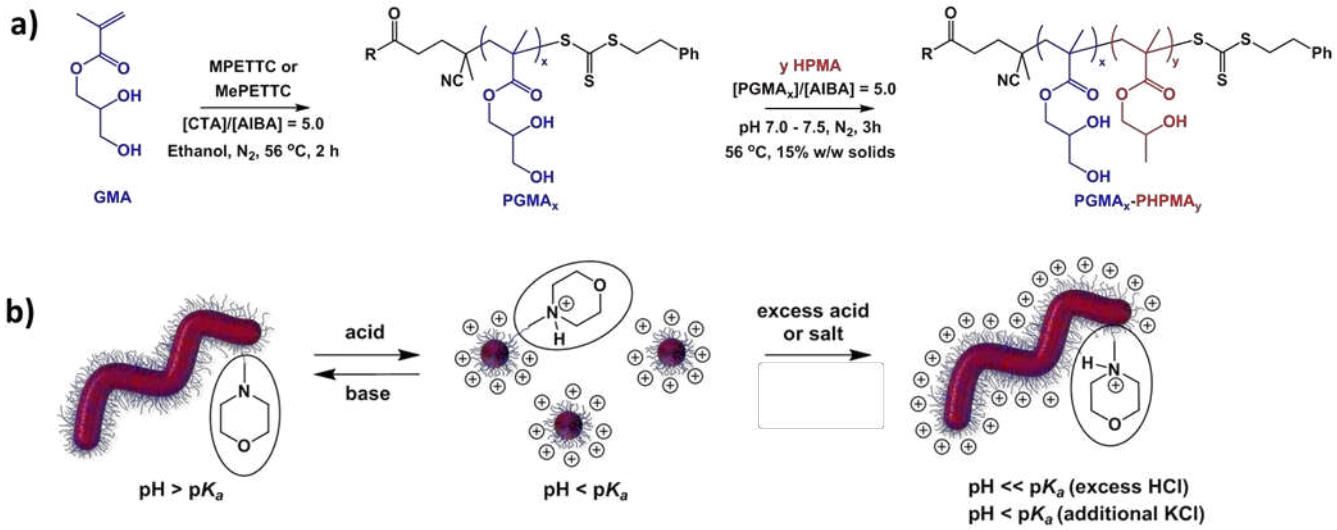

Scheme 2. Schematic representation of (a) synthesis of a $PGMA_X$ macro-CTA by RAFT solution polymerisation of GMA (using either MPETTC or MePETTC RAFT chain transfer agent, respectively) and its subsequent chain extension with HPMA by RAFT aqueous dispersion polymerisation at pH 7.0 – 7.5 to form PGMAx-PHPMAy diblock copolymer nano-objects. (b) Schematic cartoon of the reversible worm-to-sphere transition that occurs when morpholine-functionalised PGMAx-PHPMAy diblock copolymer worms prepared using MPETTC undergo a pH switch upon addition of acid or base. Addition of salt to a spherical dispersion at pH 3 can also induce the sphere-to-worm transition.

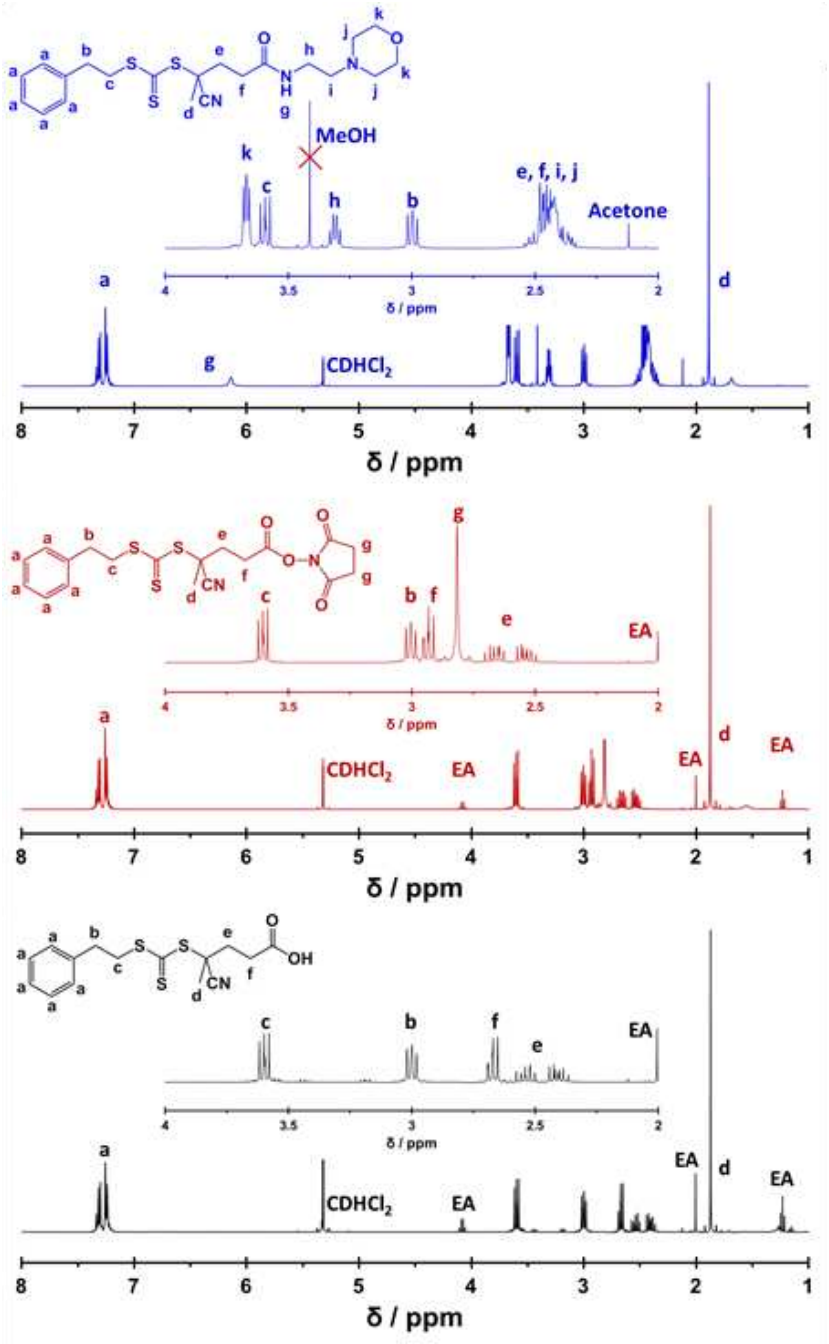

Figure 1 . ^{1}H NMR spectra recorded for PETTC (black trace), SPETTC (red trace) and MPETTC (blue trace) RAFT agents in CD_2Cl_2. The 2 – 4 ppm region is expanded to indicate proton splitting patterns. 'EA' and 'MeOH' denotes traces of ethyl acetate and methanol, respectively.

Successful conjugation of *N*-hydroxylsuccinimide was confirmed by the appearance of a four-proton singlet at 2.82 ppm (relative to the five aromatic protons lying between 7.22 and 7.42 ppm). A small downfield shift in signals e and f (Figure 1, red trace) was also observed, as expected. Under the same reaction conditions described by Bathfield and co-workers[63] a 4-(2-aminoethyl) morpholine solution in anhydrous $CHCl_3$ was added to a SPETTC solution in $CHCl_3$, and heated at 30 ^{o}C for 90 minutes to produce MPETTC (see Scheme 1b) in a 89% yield. Formation of MPETTC was confirmed by the appearance of a triplet between 3.64 and 3.78 ppm (k), a quartet between 3.27 and 3.34 ppm (h) and

a multiplet between 2.31 and 2.55 ppm (i, j) (see Figure 1, blue trace). Time of flight electrospray mass spectroscopy confirmed the absence of any PETTC or SPETTC impurities in the final purified MPETTC. ^{13}C NMR spectroscopy also indicated successful attachment of the 4-(2-aminoethyl) morpholine moiety (see ESI, Figures S1-S3). MPETTC is soluble in water at low pH owing to protonation of its morpholine group (see ESI, Figure S4).

The MPETTC RAFT agent was subsequently used for the RAFT solution polymerisation of GMA in either water at pH 4 (see ESI, Figure S5) or in ethanol. Well defined PGMA macro-CTAs were obtained in both cases but the ethanol-synthesised macro-CTA was used for subsequent aqueous dispersion polymerisation syntheses since this protocol ensured that the morpholine end-group was present in its neutral (rather than protonated) form. The RAFT solution polymerisation of GMA in ethanol with MPETTC at 56 °C was also studied by ^{1}H NMR and DMF GPC to assess the kinetics of monomer conversion and the evolution of molecular weight, respectively (Figure 2). A mean DP of 70 was targeted at 15% w/w solids using a [MPETTC]/[AIBA] molar ratio of 5.0. Monomer conversions were calculated by comparing the integrated MPETTC aromatic end-group signals at 7.2-7.4 ppm to that of the vinyl monomer signals at 5.6 and 6.1 ppm.

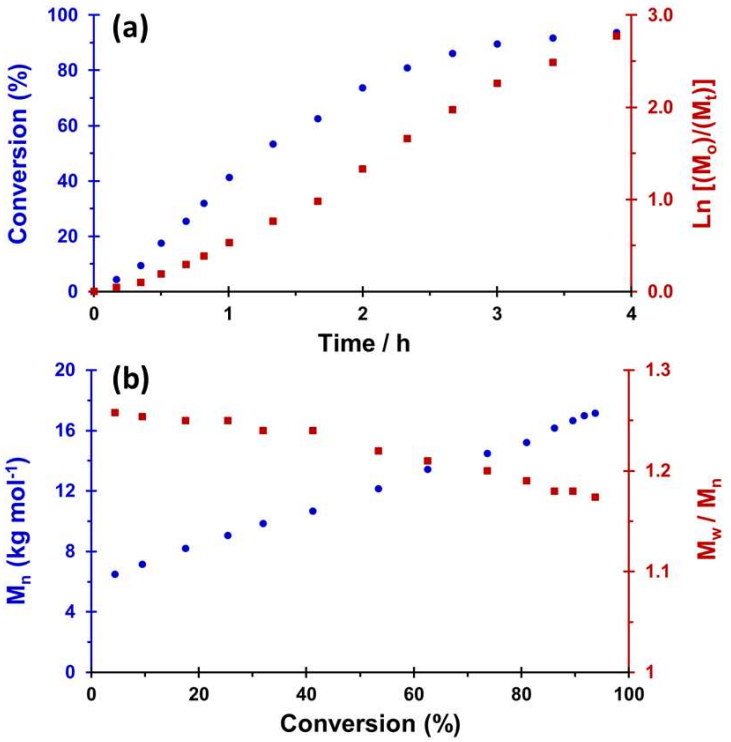

Figure 2 (a) Monomer conversion vs. time and (b) number-average molecular weight (M_n) and polydispersity (M_w/M_n) vs. conversion plots as determined by ^{1}H NMR and DMF GPC analyses, respectively, for the RAFT solution polymerisation of glycerol monomethacrylate in ethanol at 56 °C. Conditions: 45% w/w solids; target DP = 70; [MPETTC]/[AIBA] molar ratio = 5.0. M_w and M_n values were determined by DMF GPC calibrated with a series of ten near-monodisperse poly(methyl methacrylate) standards.

^{1}H NMR analysis indicated a GMA conversion of 74% within 2 h, with essentially full conversion being achieved after 6 h. A linear semi-logarithmic plot against time indicated first-order kinetics with respect to monomer concentration.

Similarly, the linear evolution in polymer molecular weight, M_n, with monomer conversion, confirmed the expected pseudo-living character of this RAFT solution polymerisation (Figure 2). The RAFT agent efficiency was estimated to be 84%, which is comparable to previously reported data for the PETTC RAFT agent.[65]

Having established the kinetics for GMA homopolymerisation, a large batch of $PGMA_{50}$ macro-CTA containing a terminal morpholine functional group was prepared using MPETTC. DMF GPC analysis indicated an M_n of 12,800 g mol^{-1} and a relatively low final M_w/M_n of 1.20 (see ESI, Figure S6a). Acid titration studies indicated that the pK_a for this MPETTC-$PGMA_{50}$ precursor is approximately 6.3 (see ESI, Figure S7). This water-soluble $PGMA_{50}$ macro-CTA was then chain-extended via RAFT aqueous dispersion polymerisation of HPMA at 56 °C and 15% w/w solids (target PHPMA DP = 140). The solution pH was adjusted to pH 7.0-7.5 prior to polymerisation to ensure that the morpholine end-group remained in its neutral free amine form. ^{1}H NMR spectroscopy studies indicated more than 99 % monomer conversion by comparing the integrated methacrylic backbone signal to that of the monomer vinyl signals. DMF GPC studies indicated a relatively low final polydispersity (M_w/M_n = 1.14) and a relatively high blocking efficiency for the MPETTC-$PGMA_{50}$ macro-CTA (see ESI, Figure S6a). TEM studies confirmed the presence of MPETTC-$PGMA_{50}$-$PHPMA_{140}$ diblock copolymer worms at pH 7.0-7.5, which formed soft transparent gels at15% w/w solids (Figure 5a).

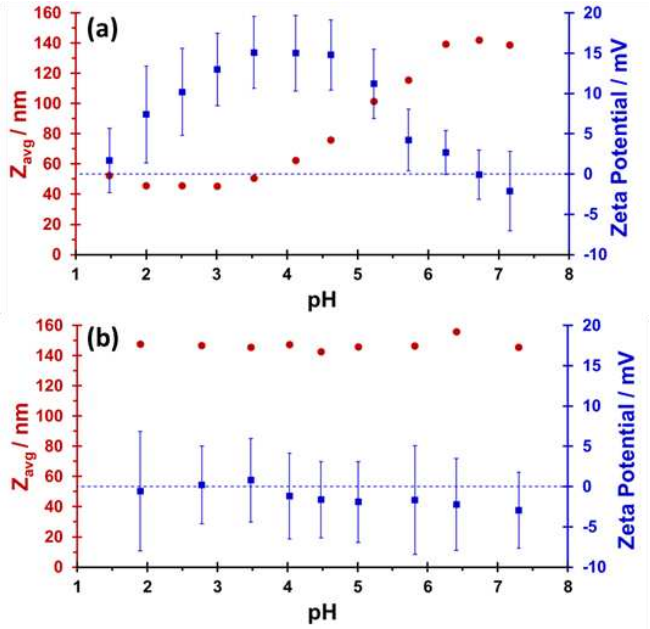

Figure 3 Hydrodynamic diameter vs. pH and zeta potential vs. pH curves obtained for (a) MPETTC-$PGMA_{50}$-$PHPMA_{140}$ and (b) MePETTC-$PGMA_{58}$-$PHPMA_{160}$ diblock copolymer nano-objects synthesised by RAFT aqueous dispersion polymerisation of HPMA at pH 7.0-7.5. Measurements are reported for 0.1% w/w copolymer dispersions prepared in the presence of 1 mM KCl. All pH titrations were performed from high pH to low pH. Error bars for zeta potential data are equivalent to 1 standard deviation.

For control experiments, the carboxylic acid functional group of PETTC was exhaustively methylated according to previous protocol in order to produce non-ionic RAFT agent, MePETTC.[61] A $PGMA_{58}$ macro-CTA was prepared using MePETTC via RAFT solution polymerisation of GMA in ethanol. DMF GPC indicated an M_n of 14,600 g mol^{-1} and a final M_w/M_n of 1.23 (see ESI, Figure S6b). This non-ionic $PGMA_{58}$ macro-CTA was chain-extended with HPMA (target DP =

160) at 15% w/w solids via RAFT aqueous dispersion polymerisation at pH 7.0-7.5. ^{1}H NMR spectroscopy studies indicated more than 99 % monomer conversion within 4 h, while DMF GPC studies indicated a relatively low final polydispersity (M_w/M_n < 1.20) and a high blocking efficiency for the MePETTC-PGMA$_{58}$ macro-CTA (see ESI, Figure S6b). TEM studies confirmed the presence of worms which formed soft, free-standing gels at pH 7.0-7.5 and 15% w/w solids (see ESI, Figure S8).

Dynamic light scattering and aqueous electrophoresis experiments were performed to examine the effect of pH on the apparent particle size and zeta potential of MPETTC-PGMA$_{50}$-PHPMA$_{140}$ and MePETTC-PGMA$_{58}$-PHPMA$_{160}$ diblock copolymer worms, respectively (Figure 3). Intensity-average hydrodynamic diameters are calculated via the Stokes-Einstein equation. Hence a 'sphere-equivalent' diameter is reported in the case of diblock copolymer worms, which represents neither the mean worm length nor the mean worm width. For MPETTC-PGMA$_{50}$-PHPMA$_{140}$ block copolymer nano-objects, a significant reduction in apparent particle size from 139 nm to 43 nm is observed, while a concomitant increase in zeta potential from approximately 0 mV to +15 mV occurs on lowering the solution pH from 7 to 3.

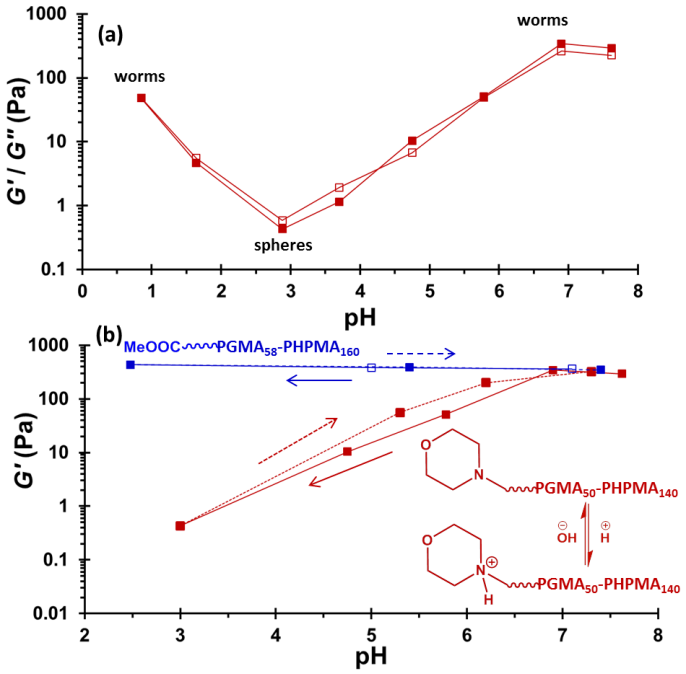

Figure 4. (a) Variation in *G'* (filled squares) and *G''* (open squares) with respect to pH for MPETTC-PGMA$_{50}$-PHPMA$_{140}$ diblock copolymer nano-objects at 15% w/w solids after switching from pH 7.6 to pH 0.9. (b) Variation in *G'* for the same MPETTC-PGMA$_{50}$-PHPMA$_{140}$ diblock copolymer nano-objects on lowering the solution pH from pH 6.8 to pH 3.0 (solid red line) and returning from pH 3.0 to pH 7.3 (red dotted line). Similar pH switch experiments conducted on a control sample of MePETTC-PGMA$_{58}$-PHPMA$_{160}$ diblock copolymer worms from pH 7.1 to pH 2.5 (blue solid line) and returning to pH 7.8 (blue dotted line). For the former worm gel, there is a reversible worm-to-sphere-worm transition mediated via protonation of the morpholine end-groups located on the PGMA stabiliser blocks. In contrast, no pH-responsive behaviour is observed for the latter worm gel, since these copolymer chains do not contain suitable end-groups.

A reduction in hydrodynamic diameter is observed as the MPETTC-PGMA$_{50}$-PHPMA$_{140}$ morpholine end-group becomes protonated below its pK_a of 6.27, since the resulting terminal cationic charge increases the degree of hydration of the PGMA stabiliser block. This reduces the packing parameter, *P*, which in turn induces a worm-to-sphere transition.[31, 66] A reduction in zeta potential to around 0 mV is observed at pH ~ 1 because excess HCl acts as a salt, hence screening the cationic charge arising from the protonated morpholine groups. This observation, together with a modest increase in the intensity-average hydrodynamic diameter, suggests that worm reformation might be feasible, but efficient fusion of multiple spheres to form worms[67] is unlikely to occur on normal experimental time scales at high dilution (i.e. for the 0.1% w/w copolymer dispersions required for DLS and electrophoresis studies). MePETTC-PGMA$_{58}$-PHPMA$_{160}$ block copolymer worms exhibit no appreciable change in either apparent size (≈ 145 nm) or zeta potential (≈ 0 mV) on adjusting the solution pH, as expected.

Rheological studies (Figure 4a) were performed at 20 °C as a function of pH on both the cationic MPETTC-PGMA$_{50}$-PHPMA$_{140}$ and non-ionic MePETTC-PGMA$_{58}$-PHPMA$_{160}$ diblock copolymer worm gels at 15% w/w solids. The former worm gel exhibits a maximum *G'* of 342 Pa at pH 6.8. Upon lowering the solution pH to pH 3, a dramatic reduction in *G'* to just 0.40 Pa was observed. In addition, *G''* exceeds *G'* at pH 3, confirming degelation.

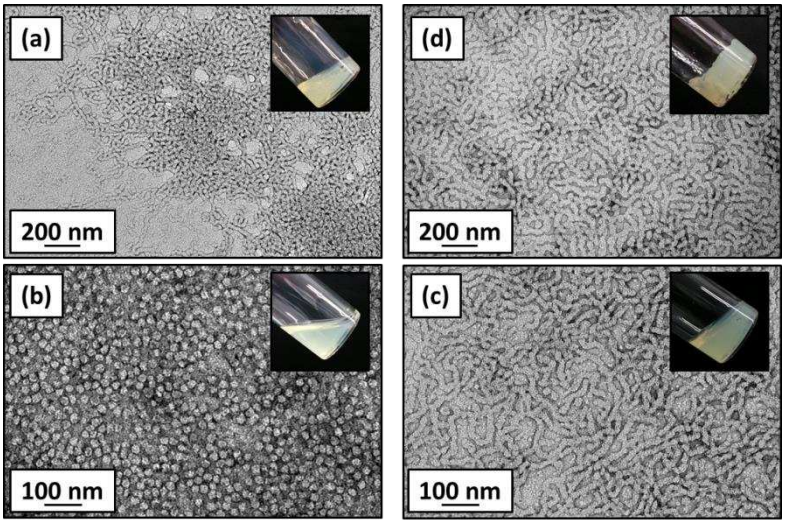

Figure 5 TEM images and corresponding digital photographs obtained for MPETTC-PGMA$_{50}$-PHPMA$_{140}$ diblock copolymer nano-objects prepared via RAFT aqueous dispersion polymerisation of HPMA: (a) pH 7.2, (b) pH 3.0, (c) pH 0.9 and (d) after a pH switch from pH 7.2 to 3.0 to 7.3. A worm-to-sphere transition is observed on lowering the dispersion pH from 7.2 to 3.0. Further reduction in pH to 0.9 induces a sphere-to-worm transition, as excess acid acts as a salt.

Corresponding TEM studies indicate a change in copolymer morphology from worms at pH 7 to exclusively spheres at pH 3 (Figure 5b). Furthermore, lowering the solution pH below 3 had a dramatic effect on the worm gel strength. Excess HCl acts as a salt and hence shields the cationic charge density due to the morpholine end-groups, thus inducing a sphere-to-worm morphological transition. Thus fusion of multiple spheres is feasible at sufficiently high copolymer concentrations of (e.g. 15% w/w solids) and regelation is observed at pH 0.9. However, in this case the *G'* of the reconstituted worm gel is significantly weaker than the original gel (48 Pa

vs. 342 Pa). TEM studies undertaken on dispersions dried at pH 0.9 indicate that worms are the exclusive morphology (Figure 5d). One possible explanation is that the mean contour length of the reconstituted worms is significantly shorter than that of the original worms, which would necessarily reduce the number of inter-worm contacts. Alternatively, the reconstituted worms may regain their original mean contour length but the inter-worm attractive interactions may be significantly weaker because each worm possesses residual cationic character (electrostatic screening over longer length scales may not be effective over shorter length scales). DLS studies were conducted on the reconstituted worms at pH 1. The sphere-equivalent diameter of 161 nm is actually *larger* than the original diameter of 139 nm, suggesting the formation of somewhat longer worms at low pH. Hence the reconstituted worm gels are most likely weaker because each worm possesses residual cationic character, which leads to inter-worm repulsion. In contrast, the original gel strength can be regained via a pH sweep from pH 6.8 to pH 3.0 and back to pH 7.3 (Figure 4b, red trace). Deprotonation of the morpholine end-group occurs as the solution pH increases from 3.0 to 7.3, inducing a sphere-to-worm transition at high copolymer concentrations. DLS studies indicate a spherical-equivalent diameter of 140 nm for the reconstituted worms. This is almost identical to that observed for the original worms (139 nm diameter), suggesting comparable mean worm contour lengths.

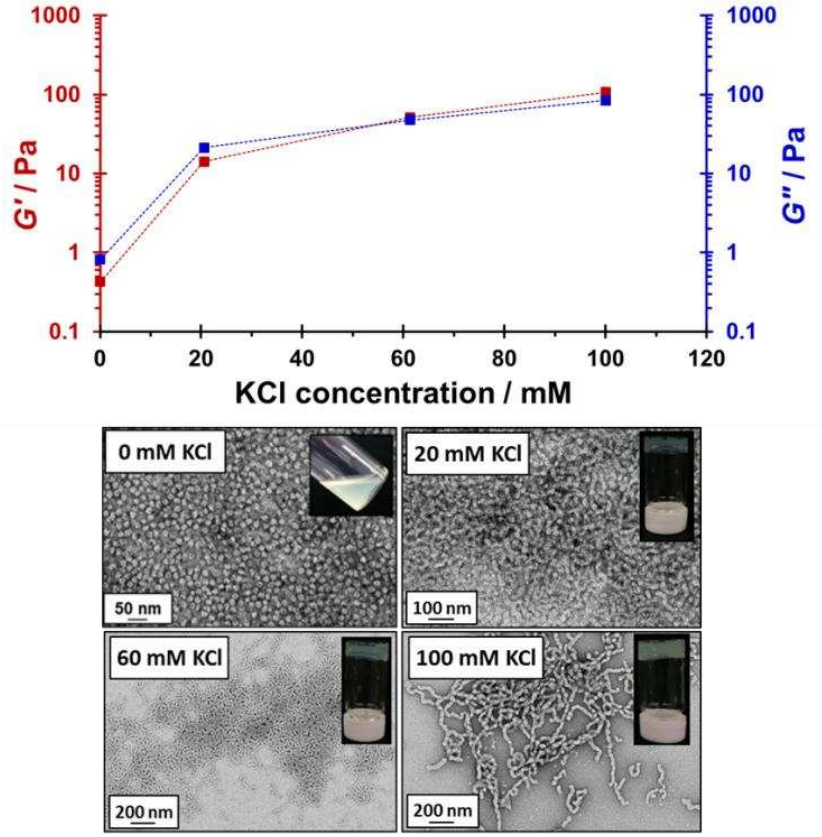

Figure 6 Variation in the gel storage modulus (*G'*) and loss modulus (*G''*) with corresponding TEM images, with respect to KCl concentration, for a pH 3 spherical dispersion of MPETTC-PGMA$_{50}$-PHPMA$_{140}$ diblock copolymer nano-objects. Rheological experiments were conducted at 15% w/w and 20 ^{o}C with 1% strain and an angular frequency of 1 rad s^{-1}.

Under these conditions, the reconstituted worm gel is comparable to the original worm gel (321 Pa vs. 342 Pa), which suggests similar mean worm contour lengths, and a comparable number of inter-worm contacts. TEM indicates that

the reconstituted gel comprises exclusively worms, rather than a mixture of worms and spheres (Figure 5). In control experiments, the MePETTC-PGMA$_{58}$-PHPMA$_{160}$ diblock copolymer worm gel remains unchanged on lowering the solution pH, as the methyl ester end-groups located on the conditions PGMA chain-ends are pH-insensitive. Hence, there can be no change in the packing parameter, *P*, under these and consequently no worm-to-sphere transition (Figure 4b, blue trace). As expected, TEM studies undertaken at various solution pH confirm that MePETTC-PGMA$_{58}$-PHPMA$_{160}$ diblock copolymer worms undergo no change in morphology (see ESI, Figure S8). Both MPETTC-PGMA$_{50}$-PHPMA$_{140}$ and MePETTC-PGMA$_{58}$-PHPMA$_{160}$ diblock copolymer worms undergo reversible degelation at pH 7 upon cooling to 4 °C, as judged by the tube inversion test.[48]

TEM and oscillatory rheology studies (Figure 6) were conducted in order to study the effect of added salt on the diblock copolymer morphology and gel strength. In these experiments, varying amounts of KCl were added to a 15% w/w free-flowing dispersion of cationic MPETTC-PGMA$_{50}$-PHPMA$_{140}$ *spheres* at pH 3. At a relatively low salt concentration (20 mM KCl), there is a substantial increase in viscosity, with *G'* increasing by an order of magnitude up to 14 Pa. However, *G'* still remained below *G"* (21 Pa), indicating that the dispersion was merely a viscous liquid, rather than a genuine gel under these conditions. Nevertheless, TEM studies indicate the presence of dimers, trimers and/or short worms, suggesting at least partial fusion of spheres. A further increase in viscosity was observed at 60 mM KCl (as judged by the tube inversion test, see Figure 6). In this case *G'* exceeded *G"* (52 Pa vs. 47 Pa, respectively), indicating formation of a genuine gel. The corresponding TEM images indicated that the copolymer morphology comprised relatively long worms under these conditions, see Figure 6. A further increase in KCl concentration up to 100 mM produced a *G*' of 107 Pa, but the original gel modulus of 342 Pa could not be regained. We hypothesise that this is because the protonated cationic morpholine end-groups expressed at the worm periphery leads to weaker and/or fewer inter-worm contacts. These findings agree with previous work by Geng *et al.*, who found that the addition of salt to diblock copolymer spheres at constant pH led to the formation of cylindrical diblock copolymers.[68]

Conclusions

In summary, a carboxylic acid-based RAFT agent (PETTC) was reacted with 4-(2-aminoethyl)morpholine to yield a new morpholine-functionalised RAFT agent (MPETTC) in a two-step protocol.[63] MPETTC is soluble in acidic solution, which allows the convenient synthesis of a well-defined PGMA$_{75}$ macro-CTA directly in water. Alternatively, a morpholine-functionalised PGMA$_{50}$ macro-CTA was also prepared by RAFT solution polymerisation of GMA in ethanol to maintain the neutral character of the morpholine end-group. Chain extension of this latter PGMA$_{50}$ macro-CTA via RAFT aqueous dispersion polymerisation of HPMA at pH 7.0-7.5 produced PGMA$_{50}$-PHPMA$_{140}$ diblock copolymer worms via polymerisation-induced self-assembly. These worms formed soft free-standing gels, as judged by rheological studies. Protonation of the morpholine end-group on addition of HCl induced a PGMA$_{50}$-PHPMA$_{140}$ worm-to-sphere morphological transition, causing complete degelation to occur at pH 3. However, *further reduction* of the solution pH leads to reformation of a worm gel. This is because the excess HCl acts as a salt, thus screening the effect of the cationic charge located at the end of each PGMA chain. Furthermore, the addition of salt at pH 3 can also cause a sphere-to-worm transition, although the original gel modulus is not recovered in this case. These order-order transitions driven by end-group protonation constitute complementary pH-responsive behaviour to that recently reported by Lovett et al.[61] for carboxylic acid-functionalised diblock copolymer worms.

Acknowledgements

Svetomir Tzokov is thanked for carbon coating the TEM grids. SPA acknowledges an ERC Advanced Investigator grant (PISA 320273). EPSRC and P & G are thanked for supporting a CASE PhD studentship for NJWP.

References

1. R. C. Hayward and D. J. Pochan, *Macromolecules*, 2010, **43**, 3577-3584.
2. Z. Tuzar and P. Kratochvil, *Advances in Colloid and Interface Science*, 1976, **6**, 201-232.
3. L. Zhang and A. Eisenberg, *Science*, 1995, **268**, 1728-1731.
4. Z. Li, E. Kesselman, Y. Talmon, M. A. Hillmyer and T. P. Lodge, *Science*, 2004, **306**, 98-101.
5. D. J. Pochan, Z. Chen, H. Cui, K. Hales, K. Qi and K. L. Wooley, *Science*, 2004, **306**, 94-97.
6. H. Cui, Z. Chen, S. Zhong, K. L. Wooley and D. J. Pochan, *Science*, 2007, **317**, 647-650.
7. J. A. Zupancich, F. S. Bates and M. A. Hillmyer, *Macromolecules*, 2006, **39**, 4286-4288.
8. S. Jain and F. S. Bates, *Macromolecules*, 2004, **37**, 1511-1523.
9. Y.-Y. Won, H. T. Davis and F. S. Bates, *Macromolecules*, 2003, **36**, 953-955.
10. H. Bermudez, A. K. Brannan, D. A. Hammer, F. S. Bates and D. E. Discher, *Macromolecules*, 2002, **35**, 8203-8208.
11. S. Jain and F. S. Bates, *Science*, 2003, **300**, 460-464.
12. J. A. Zupancich, F. S. Bates and M. A. Hillmyer, *Biomacromolecules*, 2009, **10**, 1554-1563.
13. A. B. Lowe, B. S. Sumerlin, M. S. Donovan and C. L. McCormick, *Journal of the American Chemical Society*, 2002, **124**, 11562-11563.
14. M. S. Donovan, A. B. Lowe, B. S. Sumerlin and C. L. McCormick, *Macromolecules*, 2002, **35**, 4123-4132.
15. B. S. Sumerlin, A. B. Lowe, D. B. Thomas and C. L. McCormick, *Macromolecules*, 2003, **36**, 5982-5987.
16. C. L. McCormick, B. S. Sumerlin, B. S. Lokitz and J. E. Stempka, *Soft Matter*, 2008, **4**, 1760-1773.
17. R. K. O'Reilly, M. J. Joralemon, C. J. Hawker and K. L. Wooley, *Journal of Polymer Science Part A: Polymer Chemistry*, 2006, **44**, 5203-5217.
18. J. Bang, S. H. Kim, E. Drockenmuller, M. J. Misner, T. P. Russell and C. J. Hawker, *Journal of the American Chemical Society*, 2006, **128**, 7622-7629.
19. R. J. Amir, S. Zhong, D. J. Pochan and C. J. Hawker, *Journal of the American Chemical Society*, 2009, **131**, 13949-13951.
20. S.-Y. Ku, M. A. Brady, N. D. Treat, J. E. Cochran, M. J. Robb, E. J. Kramer, M. L. Chabinyc and C. J. Hawker, *Journal of the American Chemical Society*, 2012, **134**, 16040-16046.
21. J.-S. Wang and K. Matyjaszewski, *Journal of the American Chemical Society*, 1995, **117**, 5614-5615.
22. M. Kato, M. Kamigaito, M. Sawamoto and T. Higashimura, *Macromolecules*, 1995, **28**, 1721-1723.
23. J. Chiefari, Y. K. Chong, F. Ercole, J. Krstina, J. Jeffery, T. P. T. Le, R. T. A. Mayadunne, G. F. Meijs, C. L. Moad, G. Moad, E. Rizzardo and S. H. Thang, *Macromolecules*, 1998, **31**, 5559-5562.
24. M. Semsarilar, E. R. Jones and S. P. Armes, *Polymer Chemistry*, 2014, **5**, 195-203.

25. Q. Ma and K. L. Wooley, *Journal of Polymer Science Part A: Polymer Chemistry*, 2000, **38**, 4805-4820.

26. Y. Li and S. P. Armes, *Angewandte Chemie International Edition*, 2010, **49**, 4042-4046.

27. V. J. Cunningham, A. M. Alswieleh, K. L. Thompson, M. Williams, G. J. Leggett, S. P. Armes and O. M. Musa, *Macromolecules*, 2014, **47**, 5613-5623.

28. S. Binauld, L. Delafresnaye, B. Charleux, F. D'Agosto and M. Lansalot, *Macromolecules*, 2014, **47**, 3461-3472.

29. B. T. T. Pham, D. Nguyen, C. J. Ferguson, B. S. Hawkett, A. K. Serelis and C. H. Such, *Macromolecules*, 2003, **36**, 8907-8909.

30. C. J. Ferguson, R. J. Hughes, D. Nguyen, B. T. T. Pham, R. G. Gilbert, A. K. Serelis, C. H. Such and B. S. Hawkett, *Macromolecules*, 2005, **38**, 2191-2204.

31. A. Blanazs, S. P. Armes and A. J. Ryan, *Macromolecular rapid communications*, 2009, **30**, 267-277.

32. A. Blanazs, A. J. Ryan and S. P. Armes, *Macromolecules*, 2012, **45**, 5099-5107.

33. I. Chaduc, A. Crepet, O. Boyron, B. Charleux, F. D'Agosto and M. Lansalot, *Macromolecules*, 2013, **46**, 6013-6023.

34. W. Zhang, F. D'Agosto, O. Boyron, J. Rieger and B. Charleux, *Macromolecules*, 2011, **44**, 7584-7593.

35. X. Zhang, S. Boisse, W. Zhang, P. Beaunier, F. D'Agosto, J. Rieger and B. Charleux, *Macromolecules* 2011, **44**, 4149-4158.

36. S. Boisse, J. Rieger, K. Belal, A. Di-Cicco, P. Beaunier, M.-H. Li and B. Charleux, *Chemical Communications*, 2010, **46**, 1950-1952.

37. W. Zhang, F. D'Agosto, O. Boyron, J. Rieger and B. Charleux, *Macromolecules*, 2012, **45**, 4075-4084.

38. N. J. Warren and S. P. Armes, *Journal of the American Chemical Society*, 2014, **136**, 10174-10185.

39. N. J. Warren, O. O. Mykhaylyk, D. Mahmood, A. J. Ryan and S. P. Armes, *Journal of the American Chemical Society*, 2014, **136**, 1023-1033.

40. M. Semsarilar, V. Ladmiral, A. Blanazs and S. P. Armes, *Langmuir : the ACS journal of surfaces and colloids*, 2012, **28**, 914-922.

41. M. Semsarilar, V. Ladmiral, A. Blanazs and S. P. Armes, *Langmuir : the ACS journal of surfaces and colloids*, 2013, **29**, 7416-7424.

42. B. Charleux, G. Delaittre, J. Rieger and F. D'Agosto, *Macromolecules*, 2012, **45**, 6753-6765.

43. V. Ladmiral, M. Semsarilar, I. Canton and S. P. Armes, *Journal of the American Chemical Society*, 2013, **135**, 13574-13581.

44. V. Ladmiral, A. Charlot, M. Semsarilar and S. P. Armes, *Polymer Chemistry*, 2015, **6**, 1805-1816.

45. S. Sugihara, A. Blanazs, S. P. Armes, A. J. Ryan and A. L. Lewis, *Journal of the American Chemical Society*, 2011, **133**, 15707-15713.

46. K. E. B. Doncom, N. J. Warren and S. P. Armes, *Polymer Chemistry*, 2015, Ahead of Print.

47. R. Verber, A. Blanazs and S. P. Armes, *Soft Matter*, 2012, **8**, 9915-9922.

48. A. Blanazs, R. Verber, O. O. Mykhaylyk, A. J. Ryan, J. Z. Heath, C. W. Douglas and S. P. Armes, *Journal of the American Chemical Society*, 2012, **134**, 9741-9748.

49. E. R. Gillies and J. M. J. Frechet, *Bioconjugate Chemistry*, 2005, **16**, 361-368.

50. J. Taillefer, M. C. Jones, N. Brasseur, J. E. Van Lier and J. C. Leroux, *Journal of Pharmaceutical Sciences*, 2000, **89**, 52-62.

51. F. C. Giacomelli, P. Stepanek, C. Giacomelli, V. Schmidt, E. Jaeger, A. Jaeger and K. Ulbrich, *Soft Matter*, 2011, **7**, 9316-9325.

52. S. Liu and S. P. Armes, *Angewandte Chemie International Edition*, 2002, **41**, 1413-1416.

53. J. Rodriguez-Hernandez and S. Lecommandoux, *Journal of the American Chemical Society*, 2005, **127**, 2026-2027.

54. V. Bütün, S. Liu, J. V. M. Weaver, X. Bories-Azeau, Y. Cai and S. P. Armes, *Reactive and Functional Polymers*, 2006, **66**, 157-165.

55. Y. Cai, Y. Tang and S. P. Armes, *Macromolecules*, 2004, **37**, 9728-9737.

56. A. E. Smith, X. Xu, S. E. Kirkland-York, D. A. Savin and C. L. McCormick, *Macromolecules*, 2010, **43**, 1210-1217.

57. J. V. M. Weaver, I. Bannister, K. L. Robinson, X. Bories-Azeau, S. P. Armes, M. Smallridge and P. McKenna, *Macromolecules*, 2004, **37**, 2395-2403.

58. P. A. FitzGerald, S. Gupta, K. Wood, S. Perrier and G. G. Warr, *Langmuir,* 2014, **30**, 7986-7992.

59. Y. Xia, N. A. D. Burke and H. D. H. Stöever, *Macromolecules*, 2006, **39**, 2275-2283.

60. A. O. Moughton and R. K. O'Reilly, *Chemical Communications*, 2010, **46**, 1091-1093.

61. J. R. Lovett, N. J. Warren, L. P. D. Ratcliffe, M. K. Kocik and S. P. Armes, *Angewandte Chemie International Edition*, 2015, **54**, 1279-1283.

62. E. R. Jones, M. Semsarilar, A. Blanazs and S. P. Armes, *Macromolecules*, 2012, **45**, 5091-5098.

63. M. Bathfield, F. D'Agosto, R. Spitz, M.-T. Charreyre and T. Delair, *Journal of the American Chemical Society*, 2006, **128**, 2546-2547.

64. G. W. Anderson, J. E. Zimmerman and F. M. Callahan, *Journal of the American Chemical Society*, 1964, **86**, 1839-1842.

65. L. P. D. Ratcliffe, A. J. Ryan and S. P. Armes, *Macromolecules*, 2013, **46**, 769-777.

66. D. E. Discher and A. Eisenberg, *Science*, 2002, **297**, 967-973.

67. A. Blanazs, J. Madsen, G. Battaglia, A. J. Ryan and S. P. Armes, *Journal of the American Chemical Society*, 2011, **133**, 16581-16587.

68. Y. Geng, F. Ahmed, N. Bhasin and D. E. Discher, *J. Phys. Chem. B*, 2005, **109**, 3772-3779.